

Approved for Release by NSA on 09-11-2013 pursuant to E.O. 13526

ENERGY CASCADES IN THE BEAM-WAVE ACCELERATOR

Authors: C. L. McKinstrie
S. D. Barth

Contract: F49620-85C-0002

DISCLAIMER

This report was prepared as an account of work sponsored by an agency of the United States Government. Neither the United States Government nor any agency thereof, nor any of their employees, makes any warranty, express or implied, or assumes any legal liability or responsibility for the accuracy, completeness, or usefulness of any information, apparatus, product, or process disclosed, or represents that its use would not infringe privately owned rights. Reference herein to any specific commercial product, process, or service by trade name, trademark, manufacturer, or otherwise does not necessarily constitute or imply its endorsement, recommendation, or favoring by the United States Government or any agency thereof. The views and opinions of authors expressed herein do not necessarily state or reflect those of the United States Government or any agency thereof.

Los Alamos National Laboratory
Los Alamos, New Mexico 87545

MASTER

ENERGY CASCADING IN THE BEAT-WAVE ACCELERATOR

C. J. McKinstrie^(a) and S. H. Batha^(b)

(a) Los Alamos National Laboratory, Los Alamos, New Mexico 87545

(b) Laboratory for Laser Energetics, 250 East River Road, Rochester, New York 14623

A review is given of energy cascading in the beat-wave accelerator. The properties of the electromagnetic cascade and the corresponding plasma-wave evolution are well understood within the framework of an approximate analytic model. Based on this model, idealised laser-plasma coupling efficiencies of the order of 10% do not seem unreasonable.

1. Plasma-Wave Generation

In the plasma beat-wave accelerator [1], the plasma wave is generated by the beating of two co-linear lasers [2]. The higher-frequency laser is denoted by the subscript 1, the lower-frequency laser is denoted by the subscript 0 and the plasma wave is denoted by the subscript p . The radiation pressure of the lasers induces longitudinal plasma oscillations at the laser beat-frequency. If the incident frequencies are chosen so that the plasma wave is resonantly driven, the conservation of energy and momentum is manifested by the frequency and wavevector matching conditions

$$\omega_1 = \omega_0 + \omega_p, \quad k_1 = k_0 + k_p.$$

It follows that the phase speed of the plasma wave can be expressed in terms of the incident frequencies and wavevectors as $(\omega_1 - \omega_0)/(k_1 - k_0)$. In an underdense plasma, in which the plasma frequency is much less than the incident frequencies, this is equal to the group speed $c(1 - \omega_p^2/\omega_0^2)^{1/2}$ of the light waves. The Lorentz factor associated with the phase speed of the plasma wave is therefore equal to ω_0/ω_p . Current experiments with CO₂ lasers have $\omega_0/\omega_p \approx 10$, while a proposed device has $\omega_0/\omega_p \approx 100$.

The plasma-wave amplitude evolves according to the equation

$$\left(\frac{\partial}{\partial t} + v_p \frac{\partial}{\partial z} \right) A_p = -\omega_p A_1 A_0^* + i\alpha |A_p|^2 A_p, \quad (1)$$

where the group speed, coupling constant and nonlinear frequency-shift coefficient are given by

$$v_p = 3v_e^2/c, \quad \beta_p = c^2 k_p^2 / 4\omega_p^2, \quad \alpha = 3\omega_p^2 / c^2 k_p^2, \quad (2)$$

respectively. Time is measured in units of ω_p^{-1} and distance is measured in units of $c\omega_p^{-1}$. A_p is the peak density fluctuation associated with the plasma wave, normalized to the background density. The

corresponding electrostatic field is

$$E_p \approx 0.97(n[\text{cm}^{-3}])^{1/2} A_p$$

A_1 and A_0 are the peak "quiver" velocities of electrons in the laser fields and are related to the incident laser intensities by

$$A_i = 8.5 \times 10^{-10} \lambda_i [\mu\text{m}] (I_i [\text{Wcm}^{-2}])^{1/2}$$

In the linear regime, the plasma wave grows indefinitely. Eventually, however, the quiver velocity of electrons in the plasma-wave field becomes so large that the lowest-order relativistic corrections to the electron mass must be retained in the equations of motion. This results in a nonlinear reduction in the natural frequency of the plasma wave by an amount which is proportional to the square of the wave amplitude [3]. As a result of this relativistic frequency shift, the plasma wave is driven out of phase with the beating of the two light waves and the growth of the plasma-wave saturates. If the interaction is allowed to continue, the plasma-wave energy is fed back into the light waves and the plasma-wave amplitude decreases accordingly.

Consider the interaction of the light waves and the plasma wave at some arbitrary point ξ_0 in the plasma. Initially, the plasma wave has only noise-level amplitude. At some time τ_0 , the leading edges of the laser pulses reach the position ξ_0 . The plasma wave then starts to grow according to Eq. (1), with laser amplitudes which now depend on time. This growth continues until the relativistic frequency shift detunes the interaction, or the trailing edges of the laser pulses pass by, whichever occurs first. For times later than $\tau_0 + \tau_i$, the plasma wave oscillates freely, with the amplitude it had at time $\tau_0 + \tau_i$. To maximize the energy in the plasma wave, the laser pulse-length τ_i must be tailored to coincide with the maximum plasma-wave amplitude. This limits the energy in the incident laser pulses and, hence, the energy which can ultimately be delivered to the accelerated particles in one stage. Since the group speed of a plasma wave in a typical beat-wave plasma is essentially zero (2), the energy deposited in the plasma wave is left behind the laser pulses, which continually propagate into fresh plasma and continue the process anew.

The saturation time and saturated amplitude for a given pulse shape can be estimated by using the linear plasma-wave amplitude to determine the cumulative phase shift due to the plasma nonlinearity. Imposing the condition that the cumulative phase shift equals $\pi/2$ radians determines the saturation time and saturated amplitude as a function of the incident laser intensities and pulse shapes. The incident pulse lengths can then be chosen to coincide with the maximum plasma-wave amplitude, as discussed above. The Rosenbluth-Liu saturation time is given by

$$T_s[\omega_p^{-1}] \approx (7.4 - 20) |A_1 A_0|^{-2/3} \quad (3)$$

where the coefficient of 7.4 applies to laser amplitudes which are constant in time (square pulses) and the coefficient of 20 applies to laser amplitudes which grow linearly in time (triangular pulses). In the

latter case, A_1 and A_0 denote the peak laser amplitudes. The corresponding saturation length L_s is equal to the acceleration time multiplied by the speed of light. The saturated amplitude is given by

$$A_{max} \approx (1.8 - 1.7)[A_1 A_0]^{1/3}, \quad (4)$$

where the coefficient of 1.8 applies to square pulses and the coefficient of 1.7 applies to triangular pulses. In Eqs. (3) and (4), the weak dependence of T_s and A_{max} on ω_0/ω_p has been suppressed.

This simple theory of plasma-wave generation is in good agreement with the results of computer simulations [4], [5]. Experimental verification was first obtained by Joshi *et al.* [6]. The 9.6 μm ($A_1 \approx 0.030$) and 10.6 μm ($A_0 \approx 0.015$) lines of a CO_2 laser were used to resonantly drive a plasma wave in a plasma of density $1.1 \times 10^{17} \text{ cm}^{-3}$. The laser amplitudes were modeled as growing linearly in time for a duration of 1 ns. For these parameters, Eq. (5) predicts a *maximum* plasma-wave amplitude A_p of approximately 0.08 at the middle of the laser pulse. By measuring the time-integrated scattered light, an *average* amplitude A_p of 0.01 – 0.03 was inferred, in good agreement with the theoretical estimate. The corresponding electrostatic field was 3 – 10 MeVcm^{-1} , which marked the first time a longitudinal field in excess of 1 MeVcm^{-1} had been produced, in a controlled manner, by any means. Ebrahim *et al.* [7] have also confirmed the theory by measuring the acceleration of injected electrons. In their experiment, the 9.6 μm ($A_1 \approx 0.054$) and 10.6 μm ($A_0 \approx 0.060$) lines of a CO_2 laser were also used to resonantly drive a plasma wave in a plasma of density $1.1 \times 10^{17} \text{ cm}^{-3}$. For these parameters, theory predicts a *maximum* plasma-wave amplitude A_p of approximately 0.16 and a corresponding *maximum* electrostatic field of approximately 50 MeVcm^{-1} . The electrons were produced by irradiating an aluminum slab with an auxiliary high-intensity CO_2 laser. The energy of the electrons obtained in this manner was 0.5 – 1.0 MeV. Measurements indicated that electrons injected at 0.6 MeV were accelerated to 2.0 MeV. Since the resonant plasma region was only 0.15 cm long, this implied that the *average* electrostatic field was 10 MeVcm^{-1} , in good agreement with the theoretical estimate.

2. Long-Time Evolution

It can be seen from Eq. (3) that, for typical laser intensities ($A_l \approx 0.2$), the plasma-wave saturation time is of the order of $10^2 \omega_p^{-1}$. On this timescale, the mechanisms described in Section 1 are dominant. However, the saturation time is much shorter than the acceleration time, defined as the time taken by an accelerated particle to traverse one quarter wavelength in the wave frame. Approximating the speed of the accelerated particle by the speed of light gives an acceleration time of $\lambda_p/[4(c - v_\phi)]$. By expressing v_ϕ in terms of the frequency ratio ω_0/ω_p , this becomes

$$T_a[\omega_p^{-1}] \approx 3.1(\omega_0/\omega_p)^2. \quad (5)$$

The acceleration length L_a is the acceleration time multiplied by the speed of light and corresponds to the distance travelled by the accelerated particle during the acceleration time. For proposed beat wave

parameters, the acceleration time is of the order of $10^4 \omega_p^{-1}$. There are several processes which can occur on this longer timescale and have important consequences for the plasma-wave evolution.

Behind the laser pulses, the wake of the plasma wave becomes turbulent. This can be due to the parametric decay instability, in which the plasma wave decays into a secondary plasma wave and an ion-acoustic wave [8] – [10], or the modulational instability [11]. These instabilities both involve ion motion and occur on a timescale longer than the electron timescale ω_p^{-1} by a factor of $(m_i/Zm_e)^{1/2}$, where Z is the ionic charge. The modulational instability can also occur due to the relativistic nonlinearity in Eq. (1). The turbulent wake cannot be used for particle acceleration, and so plasma-wave generation and beam loading must be accomplished before either of these instabilities occur. Since the incident laser pulses continually propagate into fresh plasma, the deleterious effects of the ion instabilities can, in principle, be avoided. For a detailed discussion of these competing processes and the corresponding limitations on the plasma-wave growth time, the reader is referred to the papers of Mora [12] and Pesme *et al.* [13].

In the preceding analysis, the self-consistent evolution of the light-wave amplitudes was not taken into account. Just as the beating of the incident light waves produces a resonant plasma wave at the difference frequency, the beating of the transverse electron quiver-velocities with the plasma-wave density fluctuation produces oscillating currents at the sum and difference frequencies. In this way, a spectrum of co-linear light waves is generated, with frequencies and wavevectors which differ from those of the incident waves by integral multiples of ω_p and k_p respectively. In contrast to the secondary waves described above, these sidebands propagate with the incident waves and modify the process of plasma-wave generation. This nonlinear interaction can also be viewed as a series of three-wave processes in which a photon either decays into a lower-frequency photon and a plasmon, or recombines with a plasmon to produce a higher-frequency photon. Notice that the total number of photons is conserved, and so the total electromagnetic energy is proportional to the average (action-weighted) electromagnetic frequency. Notice also that the number of plasmons is equal to the difference between the number of decay interactions and the number of recombination interactions. It follows that only a fraction ω_p/ω_1 of the incident laser energy can be transferred to the plasma wave in the primary three-wave interaction [14]. For proposed beat-wave parameters, this is of the order of 1%. To increase the energy transfer to the plasma wave and ultimately to the accelerated particles, the laser energy must be made to cascade "downwards" from the incident waves to their lower-frequency sidebands.

Since the long-time evolution of the plasma wave is determined by the interaction of several competing physical processes, the natural way to study the plasma-wave evolution would seem to be using computer simulations. Unfortunately however, this approach is prohibitively expensive. From the above discussion, the plasma-wave generation, interaction with the electromagnetic sidebands and subsequent decay into secondary waves all take place in a distance of the order of the saturation length

L_s (3), measured from the front of the incident laser-pulses. Using a moving simulation code, one can save vast amounts of computer time by following this interaction region as it propagates through the plasma [15]. The simulation timestep is determined by the shortest relevant oscillation period, which, in this case, is that of the light waves. Measured relative to the plasma frequency, the simulation timestep scales as ω_0/ω_p . The plasma-wave evolution must be studied for times of the order of the interaction time T_a , which scales as $(\omega_0/\omega_p)^2$. It follows that the total cost of simulating the plasma-wave evolution scales as $(\omega_0/\omega_p)^3$. A reference simulation of experimental parameters takes about 1 Cray-hour [16]. A simulation of proposed parameters would therefore take of the order of 10^3 Cray-hours, which is much too expensive for exploratory physics. For this reason, much effort has been devoted to analysing the relevant amplitude equations.

Neglecting ion effects, the governing equations are

$$\begin{aligned} \left(\frac{\partial}{\partial t} + v_m \frac{\partial}{\partial x} \right) A_m &= -i\beta_m (A_{m+1} A_p^* \exp(-i\delta_{m+1}t) + A_{m-1} A_p \exp(i\delta_m t)) , \\ \left(\frac{\partial}{\partial t} + v_p \frac{\partial}{\partial x} + \nu \right) A_p &= -i\beta_p \sum_m A_m A_{m-1}^* \exp(-i\delta_m t) + i\alpha |A_p|^2 A_p , \end{aligned} \quad (6)$$

where the A_m are the quiver velocities of the electrons in the fields of the electromagnetic sidebands. The plasma-wave damping coefficient, and the electromagnetic group speeds and coupling constants are given by

$$\nu = \nu_e/2\omega_p , \quad v_m = c(1 - \omega_p^2/\omega_m^2)^{1/2} , \quad \beta_m = \omega_p/4\omega_m , \quad (7)$$

respectively. The wavevector \mathbf{k}_m of the m th sideband is equal to $\mathbf{k}_0 + m(\mathbf{k}_1 - \mathbf{k}_0)$. However, due to dispersion, the driven frequency $\omega_0 + m(\omega_1 - \omega_0)$ is not equal to ω_m , the natural frequency $(\omega_p^2 + c^2 k_m^2)^{1/2}$ of the m th sideband. The frequency-mismatch coefficients

$$\delta_m = (\omega_m - \omega_{m-1} - \omega_p)/\omega_p$$

are given approximately by

$$\delta_m \approx \delta_1 + (m-1)(\omega_p/\omega_0)^3 . \quad (8)$$

Formula (8) also allows for the general case in which the beat-frequency $\omega_1 - \omega_0$ of the incident waves is not exactly equal to the plasma frequency ω_p . Since the plasma frequency depends on the electron density, this linear frequency mismatch occurs experimentally whenever the electron density is not exactly equal to the value necessary for a resonant interaction. It should be noted that the problem can also be formulated in terms of the driven frequencies and the natural wavevectors. In this case, the effects of electromagnetic dispersion manifest themselves as wavevector mismatches. This difference is purely aesthetic and does not alter the physics of the interaction.

3. Temporal Cascade

There are four main timescales which are relevant to the governing equations (6): the mismatch timescale on which the plasma-wave nonlinearity detunes the plasma wave from the beating of the incident waves, the cascading timescale on which a significant amount of energy is transferred to the sidebands of the incident waves, the damping timescale on which a significant amount of plasma-wave energy is lost to dissipation and the dephasing timescale on which electromagnetic dispersion detunes the sidebands. These four timescales depend sensitively on experimental parameters such as the plasma density and temperature, and the incident laser frequencies and intensities [17]. Some idea of the rich variety of solutions to the full spatio-temporal equations (6) is given by the solutions of the simpler temporal equations ($\partial_x = 0$). In Fig. 1, the action density $|A_p|^2/\beta_p$ of the plasma wave, normalised to the initial action density $|A_1|^2/\beta_1$ of the higher-frequency pump wave, is plotted as a function of time. For proposed beat-wave parameters, the Rosenbluth-Liu saturation time is much shorter than the time for a complete transfer of action between the higher-frequency pump wave and the plasma wave, and so the peak amplitude of the plasma wave is limited by relativistic detuning. In the absence of damping, the plasma-wave amplitude exhibits nonlinear recurrence, as shown in Fig. 1(a). When damping is included, the plasma-wave amplitude exhibits some transient nonlinear oscillations before tending to a metastable steady-state, as shown in Fig. 1(b). For experimental parameters, the time for a complete transfer of action from the higher-frequency pump wave to the plasma wave is slightly less than the Rosenbluth-Liu saturation time, and so the peak amplitude of the plasma wave is not limited by relativistic detuning. However, the evolution of the plasma-wave amplitude is highly irregular, as shown in Fig. 1(c). When damping is included, the evolution of the plasma-wave amplitude becomes even more irregular, as shown in Fig. 1(d).

Fortunately, however, the small parameter ω_p/ω_0 which makes computer simulations so expensive facilitates an approximate analytic solution to the governing equations. Cohen, Kaufman and Watson were the first to study the purely temporal (or purely spatial) equations, in the context of the beat-heating of a plasma [18]. The effects of the plasma-wave nonlinearity were not included in their analysis. Cohen, Kaufman and Watson noticed that, for the case in which ω_p/ω_0 is much less than unity and the electromagnetic energy has not spread to large values of $|m|$, the coupling constants β_m (7) are approximately equal and the dispersive contribution to the frequency-mismatch coefficients δ_m (8) can be neglected. Physically, these approximations mean that the cross-section for up-scattering is equal to the cross-section for down-scattering, and that all the sidebands are resonantly driven. By using the approximations described above, Cohen, Kaufman and Watson were able to show that

$$\frac{d}{dt} \sum_m A_m A_{m-1}^* \approx 0 . \quad (9)$$

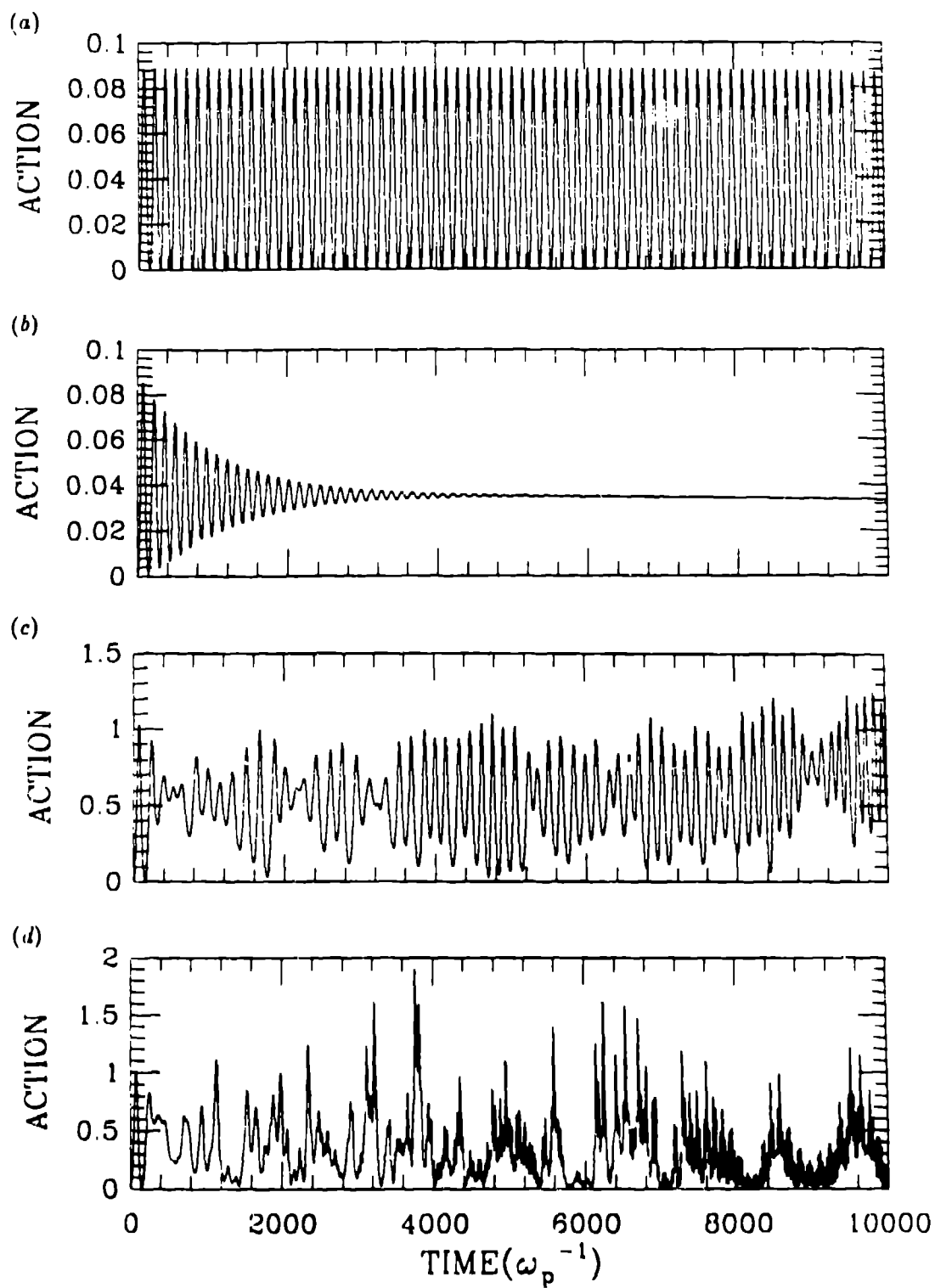


Figure 1. The action density $|A_p|^2/\beta_p$ of the plasma wave, normalised to the initial action density $|A_1|^2/\beta_1$ of the higher-frequency pump wave, is plotted as a function of time. (a) $\omega_0/\omega_p = 100$; $A_1 = A_0 = 0.2$; $\nu = 0.0$. (b) $\omega_0/\omega_p = 100$; $A_1 = A_0 = 0.2$; $\nu = 0.001$. (c) $\omega_0/\omega_p = 10$; $A_1 = A_0 = 0.2$; $\nu = 0.0$. (d) $\omega_0/\omega_p = 10$; $A_1 = A_0 = 0.2$; $\nu = 0.001$.

As the cascade develops, the plasma wave is driven not only by the beating of the incident waves, but also the beating of any pair of adjacent sidebands. Result (9) shows that the total ponderomotive force of the electromagnetic waves is constant. This decouples the plasma-wave equation from the equations which determine the evolution of the sidebands. After solving for the plasma-wave amplitude as a function of time, A_p becomes a *known* coupling term in the sideband equations, which can then be solved analytically. This approach was also used by Karttunen and Salomaa [19], [20], who included the effects of the plasma-wave nonlinearity. Given the analytic solutions to the approximate equations, one can then determine important properties of the cascade, such as how the peak amplitude of the plasma wave depends on the linear frequency mismatch δ_1 and how electromagnetic energy is shared among the sidebands. Although collisional damping plays an important role in the long-time development of the temporal cascade, it is relatively unimportant in the long-time development of the spatio-temporal cascade. Because of this lack of direct relevance to current beat-wave acceleration schemes, the effects of damping are not studied in detail.

For the purposes of beat-wave acceleration, the plasma-wave amplitude should be as large as possible. In Section 1, plasma-wave generation was discussed for the case in which the frequency matching of the incident lasers was exact. If the frequency matching is not exact, the plasma wave is detuned from the beating of the incident waves by a total frequency mismatch of $\delta_1 + \alpha|A_p|^2$. Tang, Sprangle and Sudan showed that one can partially compensate for the nonlinear detuning by using an electron density for which δ_1 is small and *negative* [21], [22]. Although the plasma wave grows more slowly in the linear regime, it stays in resonance with the incident waves for a longer time and ultimately grows to a larger amplitude. This idea has been extended by Bobin [23] and Martin *et al.* [24], who allowed the linear frequency mismatch to be a function of time. These investigations show that the plasma-wave amplitude can be increased by roughly a factor of two. However, to take full advantage of this effect, the electron density must be precisely controlled. Even if the electron density could be controlled with sufficient precision, the plasma-wave growth time is significantly longer than for exact frequency matching and the modulational instability is likely to disrupt the plasma-wave during its growth phase [25]. If one specifies a tolerable range for the peak plasma-wave amplitude and corresponding saturation time, the above analyses can be inverted to find the tolerable uncertainty in the electron density [4]. This is perhaps their most practical use. Within the framework of the approximate equations, the electromagnetic cascade is symmetric with respect to the incident frequencies. However, when the effects of electromagnetic dispersion are taken into account, the cascade can be biased “downwards”. This is because the dispersive contribution to the frequency mismatches δ_m (8) depend algebraically on the modenummer m . By arranging for δ_1 to be small and *positive*, the cascade to higher frequencies is detuned, while the cascade to lower frequencies is enhanced. Since energy is conserved, the decrease in electromagnetic energy is reflected in a larger plasma-wave amplitude. This effect, which was first noticed by Cohen, Kaufman and Watson, is in

competition with the effect of Tang, Sprangle and Sudan. However, it is only important on a timescale

$$\tau_m[\omega_p^{-1}] \approx 1.5(\omega_0/\omega_p)^3/(m-1). \quad (10)$$

This dispersion timescale depends sensitively on the rate of generation of new sidebands. It will shortly be shown that, for weakly-relativistic laser amplitudes, the dispersion timescale is longer than the acceleration timescale. This justifies the neglect of dispersion in the approximate equations.

The rate of generation of new sidebands is easily estimated. Let M be the index of the lowest-frequency sideband of any appreciable amplitude. From Eqs. (6), the amplitude A_{M-1} of the next sideband grows according to $d_t|A_{M-1}| \approx \beta_{M-1}|A_M A_p|$. By analogy with the theory of three-wave interactions, this growth can be expected to saturate when the action density $|A_{M-1}|^2/\beta_{M-1}$ of the daughter wave is of the order of the initial action density $|A_M|^2/\beta_M$ of the parent wave. This condition determines the time taken to generate the next sideband or, equivalently, the rate at which new sidebands are generated. Specifically,

$$\frac{d}{dt}M \approx -(\beta_M \beta_{M-1})^{1/2} A_p. \quad (11)$$

This cascading rate is proportional to the relevant coupling constants and the plasma-wave amplitude, as one might expect. A similar result can be derived for the cascading of energy to the higher-frequency sidebands. Using the analytic solutions of the approximate equations, Karttunen and Salomaa have estimated the cascading rate to be

$$\frac{d}{dt}M \approx -2\beta_0 A_p. \quad (12)$$

Estimates (11) and (12) agree to within a factor of two in their common regime of validity. Notice that the cascading rate depends implicitly on the linear frequency mismatch δ_1 .

The predicted properties of the electromagnetic cascade can be checked by numerically solving the exact equations. In Fig 2, the exact electromagnetic spectrum is plotted at time intervals of ten Rosenbluth-Liu oscillation periods. For laser amplitudes A_1 and A_0 of 0.2, this time interval is approximately $1.5 \times 10^3 \omega_p^{-1}$. In Fig 2(a) the cascade is symmetric with respect to the incident frequencies. This is to be expected since, for small values of $|m|$, the cross-sections for up-scattering and down-scattering are equal. The spectrum spreads by about 8 sidebands in 5 time intervals. This corresponds to a cascading rate of about $1.1 \times 10^{-3} \omega_p$. Equations (10) and (11) predict a cascading rate of about $1.5 \times 10^{-3} \omega_p$ and $0.75 \times 10^{-3} \omega_p$ respectively, in fairly good agreement with the observed rate. A reasonable estimate for the cascading time T_c , defined to be the time taken to generate all the lower-frequency sidebands, is therefore

$$T_c[\omega_p^{-1}] \approx 2.7(\omega_0/\omega_p)^2 \langle A_p \rangle^{-1}, \quad (13)$$

where $\langle \rangle$ denotes an average over the Rosenbluth-Liu oscillation period. The dependence of T_c on ω_0/ω_p and $\langle A_p \rangle$ follows from Eqs. (11) and (12), while the coefficient of 2.7 is derived from the

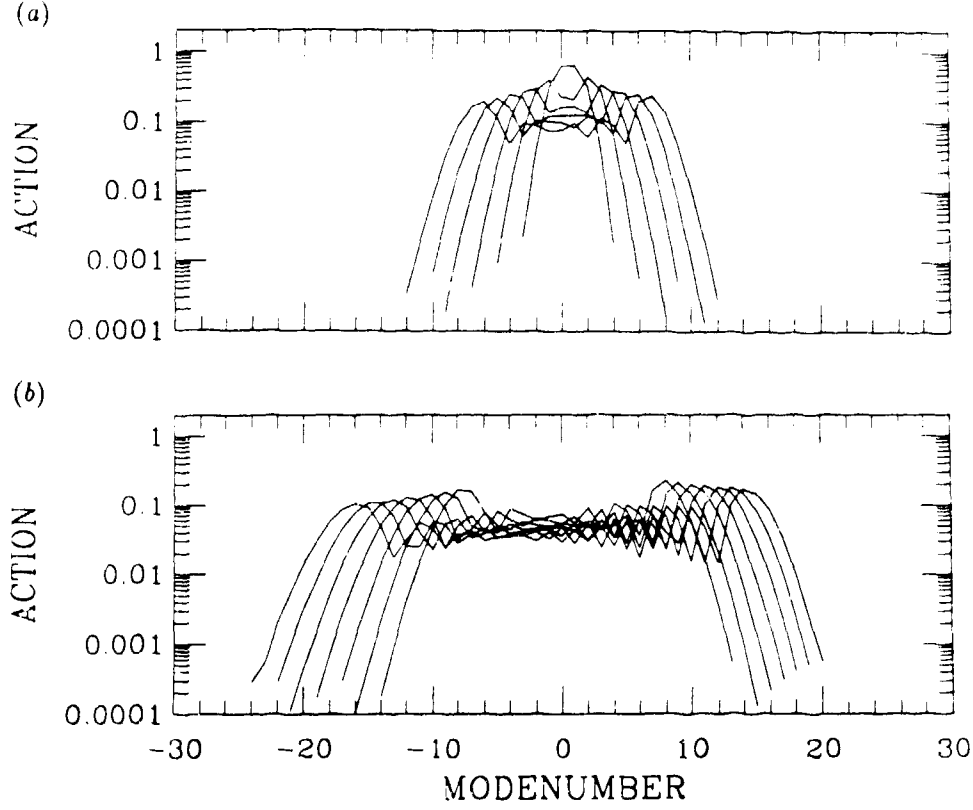


Figure 2. The action density $|A_m|^2/\beta_m$ of the electromagnetic spectrum is plotted as a function of the modenumber m . The relevant parameters are $\omega_0/\omega_p = 100$ and $A_1 = A_0 = 0.2$, and the time interval between successive spectral plots is approximately $1500\omega_p^{-1}$.

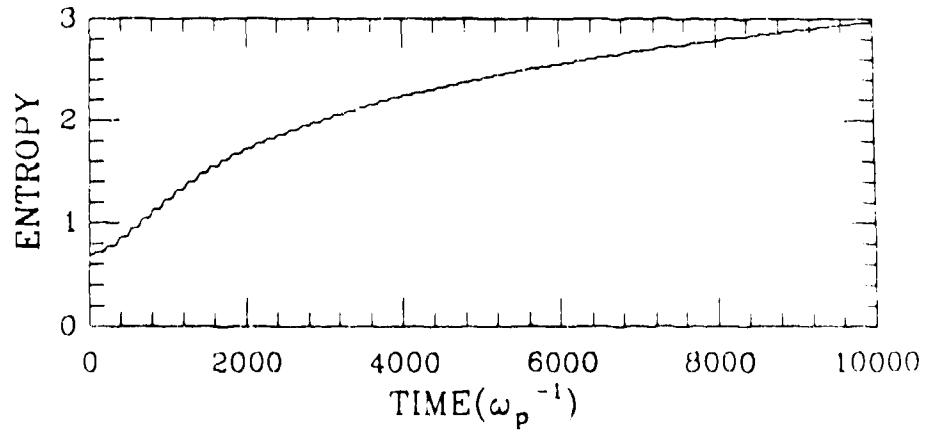


Figure 3. The entropy of the electromagnetic spectrum is plotted as a function of time. With the relative probability P_m defined as the action density of the m th mode divided by the total electromagnetic action density, the electromagnetic entropy is equal to $-\sum P_m \log P_m$.

observed cascading rate. It follows from Eqs. (5), (10) and (13) that $T_m/T_a > T_c/2T_a \approx (2.3\langle A_p \rangle)^{-1}$. For weakly-relativistic laser amplitudes, the ratio T_m/T_a is always greater than unity and so the effects of electromagnetic dispersion can be neglected on the acceleration timescale. Notice that Eq. (10) predicts that the cascade to lower frequencies should proceed more quickly and that the cascade to higher frequencies should proceed more slowly as larger values of $|m|$ are reached, in qualitative agreement with Fig. 2(b). The natural tendency of the system is to share the electromagnetic energy among the sidebands. This can be seen even more clearly in Fig. 3, in which the entropy $-\sum P_m \log P_m$ of the electromagnetic spectrum is plotted as a function of time. Apart from small fluctuations on the Rosenbluth-Liu timescale, the electromagnetic entropy increases monotonically with time.

4. Spatio-Temporal Cascade

The only qualitative difference between the temporal cascade and the spatio-temporal cascade is that, in the latter, each wave convects at its group speed as it interacts with the other waves. For the case in which ω_p/ω_0 is much less than unity, the approximations used to study the temporal cascade are also valid for the spatio-temporal cascade. In addition, the electromagnetic waves all propagate with approximately the same group speed v_0 . By using these facts, Karttunen and Salomaa [26] were able to show that

$$\left(\frac{\partial}{\partial t} + v_0 \frac{\partial}{\partial x} \right) \sum_m A_m A_{m-1}^* \approx 0.$$

This means that the total ponderomotive force of the electromagnetic waves is independent of time, *in a frame moving with the electromagnetic waves*. The driving term in the plasma-wave equation is therefore a known function of $x - v_0 t$, or equivalently, the retarded time $t - x/v_0$ measured from the leading edge of the laser pulses. After solving for the plasma-wave amplitude as a function of the retarded time, A_p becomes a known coupling term in the sideband equations, which can again be solved analytically.

For exact frequency matching, the maximum plasma-wave amplitude and corresponding saturation time are given by Eq. (4) and Eq. (3) respectively. The temporal analyses [21] – [25] of the effects of frequency mismatch are valid for the spatio-temporal problem, providing that one works in terms of the retarded time and takes the effects of laser pulse-shape into account. The estimates (11) and (12) for the cascading rate are also valid for the spatio-temporal problem. Since the cascading rate is proportional to the plasma-wave amplitude, which is now a given function of $x - v_0 t$, the electromagnetic spectrum spreads most rapidly at the trailing edge of the incident laser pulses where the plasma-wave amplitude is largest. The cascading length L_c is equal to the cascading time (13) multiplied by the speed of light, with the average plasma-wave amplitude $\langle A_p \rangle$ replaced by the maximum plasma-wave amplitude A_{\max} (4). The collisional damping of the plasma wave is only important for large values of

the retarded time. These values of the retarded time correspond to a portion of the plasma wave which is far behind the interaction region and is not coupled to the electromagnetic sidebands. It follows that the plasma-wave generation and the cascading of electromagnetic energy are unaffected by damping.

Unfortunately, the accuracy of the analytic model described above cannot be checked by comparison with numerical solutions of the exact governing equations, because such solutions do not yet exist. There is, however, a current effort to rectify this shortcoming. In the meantime, the regime of validity of the analytic model can be estimated by examining the self-consistency of the relevant approximations.

In contrast to the temporal problem, in which the peak plasma-wave amplitude has no effect on the symmetry of the electromagnetic cascade, in the spatio-temporal problem the peak plasma-wave amplitude *does* have an effect on the symmetry of the cascade. For optimal laser pulse-lengths, the rate of deposition of laser energy in the wake of the plasma wave is proportional to the square of the peak plasma-wave amplitude. This electrostatic energy is left behind the interaction region as it convects through the plasma. Since energy is conserved, there must be a corresponding decrease in electromagnetic energy and, hence, in the average electromagnetic frequency. Thus, the spatio-temporal cascade is inherently asymmetric, even for exact frequency matching. Unfortunately, neither the convective loss of electrostatic energy nor the inherent asymmetry of the cascade is self-consistently taken into account in the approximate equations. The lengthscale on which these effects become important can be easily estimated. Since the rate of energy transfer to the plasma wave is constant, the pump-depletion length L_d is determined by the requirement that the energy contained in the wake of the plasma wave is equal to the total energy which was originally contained in the laser pulses. Taking the laser pulse-lengths to be given by Eq. (3) and the plasma-wave amplitude to be given by Eq. (4), yields

$$L_d[c\omega_p^{-1}] \approx (2.2 - 2.4) \left(\frac{\omega_0}{\omega_p} \right)^2 \left(\frac{|A_1|^2 + |A_0|^2}{|A_1 A_0|^{4/3}} \right), \quad (14)$$

where the coefficient of 2.2 applies to square pulses and the coefficient of 2.4 applies to triangular pulses. By definition, this is also the lengthscale on which the average electromagnetic frequency decreases to zero. There is also a convective loss of electromagnetic energy due to the small difference in the group speeds v_m (7) of the sidebands [27]. However, this does not become important until a significant amount of energy has spread to large values of $|m|$.

It follows from the preceding analysis that there are four conditions which must be satisfied if the analytic model is to be self-consistent. The neglect of electromagnetic dispersion and the neglect of the difference in the coupling constants both require that electromagnetic energy has not spread to large values of $|m|$. This will be the case if L_a (5) is much less than L_c (13). The convective energy loss will be small compared to the incident laser energy if L_a is much less than L_d (14) and the asymmetry of the cascade will be unimportant if L_c is much less than L_d . These four constraints can be summarised

by the inequality

$$L_a \ll L_c \ll L_d . \quad (15).$$

Notice that all three lengthscales in condition (15) scale as $(\omega_0/\omega_p)^2$ and are only weakly dependent on the incident laser pulse-shapes. For the common case in which the incident laser-amplitudes are equal, the ratio L_c/L_d is approximately equal to 0.34, *independent of laser amplitude*. As a specific example, for incident laser-amplitudes of 0.06, the three lengthscales are in the ratio 1.0 : 3.4 : 10 and condition (15) is reasonably well satisfied.

The laser-plasma coupling efficiency η is defined to be the fraction of incident laser energy which is transferred to the plasma wave during the acceleration time. Since energy is deposited in the wake of the plasma wave at a constant rate, the laser-plasma coupling efficiency is given by

$$\eta \approx L_a/L_d .$$

For the specific example described above, the laser-plasma coupling efficiency is approximately 10%. In principle, the maximal laser-plasma coupling efficiency could be significantly greater than 10%. However, the approximations used in the analytic model are not valid for large values of η and so a definitive conclusion cannot be drawn at present.

5. Summary

A review was given of energy cascading in the beat-wave accelerator. The physics of the electromagnetic cascade and the corresponding plasma-wave evolution are *qualitatively* well understood. A *quantitative* analysis of these phenomena can be made using the analytic solutions of an approximate set of governing equations. For the temporal cascade, the accuracy of this approximate analytic model has been verified by comparison with numerical solutions of the exact set of governing equations. For the spatio-temporal cascade, such numerical solutions are not currently available. However, by examining the self-consistency of the relevant approximations, the regime of validity of the analytic model can be estimated.

For proposed beat-wave parameters, the effects of electromagnetic dispersion do not seem to be important on the acceleration timescale. This suggests that the plasma wave will remain coherent long enough to accelerate injected particles to high energy. In addition, idealised laser-plasma coupling efficiencies of the order of 10% do not seem unreasonable. Perhaps the most serious obstacle to the experimental realisation of such laser-plasma coupling efficiencies is the production of sufficiently-uniform plasmas. Recent progress in this direction has been reported by Dymoke-Bradshaw *et al.* [28]

Acknowledgments

This work was supported by the United States Department of Energy and by the Laser Fusion Feasibility Project at the University of Rochester.

References

- [1] T. Tajima and J. M. Dawson, *Phys. Rev. Lett.* **43**, 267 (1979)
- [2] M. N. Rosenbluth and C. S. Liu, *Phys. Rev. Lett.* **29**, 701 (1972).
- [3] A. I. Akhiezer and R. V. Polovin, *Sov. Phys. JETP* **30**, 696 (1956).
- [4] T. Katsouleas, C. Joshi, J. M. Dawson, F. F. Chen, C. E. Clayton, W. B. Mori, C. Darrow and D. Umstadter, in *Laser Acceleration of Particles*, edited by C. Joshi and T. Katsouleas, AIP Conference Proceedings 130 (American Institute of Physics, New York, 1985), p. 63.
- [5] D. W. Forslund, J. M. Kindel, W. B. Mori, C. Joshi and J. M. Dawson, *Phys. Rev. Lett.* **55**, 558 (1985).
- [6] C. Joshi, C. E. Clayton, C. Darrow and D. Umstadter, in *Laser Acceleration of Particles*, edited by C. Joshi and T. Katsouleas, AIP Conference Proceedings 130 (American Institute of Physics, New York, 1985), p. 99.
- [7] N. A. Ebrahim, F. Martin, P. Bordeur, E. A. Heighway, J. P. Matte, H. Pepin and P. Lavigne, in the *Proceedings of the 1986 Linear Accelerator Conference* (Stanford Linear Accelerator Center, Stanford, California), June 2 - 6, 1986.
- [8] D. F. DuBois and M. V. Goldman, *Phys. Rev. Lett.* **14**, 544 (1965).
- [9] D. F. DuBois and M. V. Goldman, *Phys. Rev.* **164**, 207 (1967).
- [10] V. P. Silin, *Sov. Phys. JETP* **21**, 1127 (1965).
- [11] G. B. Whitham, *Linear and Nonlinear Waves* (Wiley, New York, 1974), p. 485.
- [12] P. Mora, in these *Proceedings*.
- [13] D. Pesme, S. J. Karttunen, R. R. E. Salomaa, G. Laval and N. Sylvestre, in these *Proceedings*.
- [14] J. M. Manley and H. E. Rowe, *Proc. IRE* **40**, 904 (1956).
- [15] R. G. Evans and T. Katsouleas, in these *Proceedings*.
- [16] T. Katsouleas, private communication.
- [17] S. H. Batha and C. J. McKinstrie, *IEEE Trans. Plasma Sci.* **PS-15**, 131 (1987)
- [18] B. I. Cohen, A. N. Kaufman and K. M. Watson, *Phys. Rev. Lett.* **20**, 581 (1972)
- [19] R. R. E. Salomaa and S. J. Karttunen, *Phys. Scripta* **33**, 370 (1986).

- [20] S. J. Karttunen and R. R. E. Salomaa, *Phys. Rev. Lett.* **56**, 604 (1986).
- [21] C. M. Tang, P. Sprangle and R. N. Sudan, *Appl. Phys. Lett.* **45**, 375 (1984).
- [22] C. M. Tang, P. Sprangle and R. N. Sudan, *Phys. Fluids* **28**, 1974 (1985).
- [23] J. L. Bobin, in *Advanced Accelerator Concepts*, edited by F. E. Mills, AIP Conference Proceedings 156 (American Institute of Physics, New York, 1987), p. 105.
- [24] J. P. Matte, F. Martin, N. A. Ebrahim, P. Brodeur and H. Pepin, *IEEE Trans. Plasma Sci.* **PS-15**, 173 (1987).
- [25] C. J. McKinstrie and D. W. Forslund, *Phys. Fluids* **30**, 964 (1987).
- [26] S. J. Karttunen and R. R. E. Salomaa, *IEEE Trans. Plasma Sci.* **PS-15**, 134 (1987).
- [27] R. G. Evans, in *Laser Acceleration of Particles*, edited by C. Joshi and T. Katsouleas, AIP Conference Proceedings 130 (American Institute of Physics, New York, 1985), p. 134.
- [28] A. K. L. Dymoke-Bradshaw, A. Dyson, T. Garvey, I. Mitchell, A. J. Cole, C. N. Danson, C. B. Edwards and R. G. Evans, *IEEE Trans. Plasma Sci.* **PS-15**, 161 (1987).